Optical Measurement Systems

Laser Measurement Systems

Dawid Kucharski, PhD Eng.

Division of Metrology and Measurement Systems
Institute of Mechanical Technology
Faculty of Mechanical Engineering and Management
Poznan University of Technology

Poznan, January 3, 2018

Outline I

Outline II

Outline III

- Interferograms analysis
- Shearography image analysis
- VibroMap data analysis

Lasers

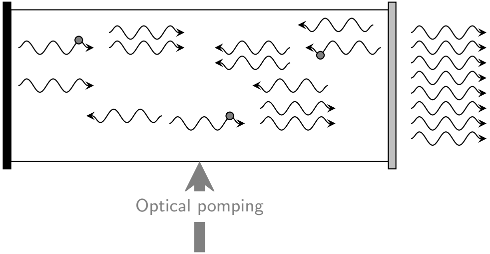

Pomping scheme

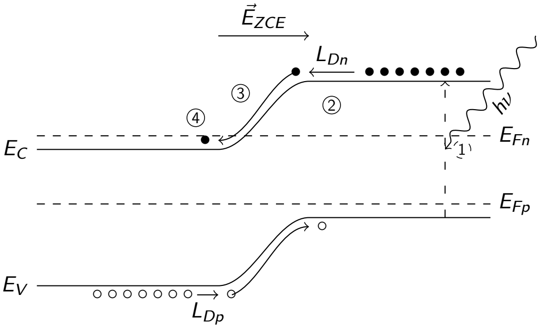

pn-junction diagram

Wave propagation

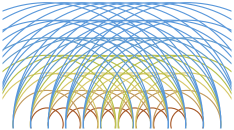

Huygens principle

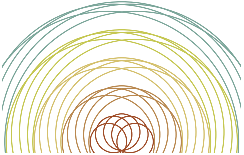

Huygens principle

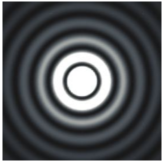

Diffraction fringes

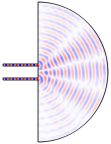

Example of diffraction

Wave propagation

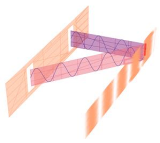

Interference phenomena

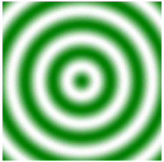

Interference fringes

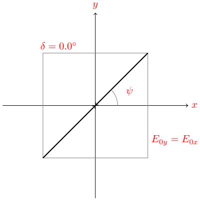

Linear pol.

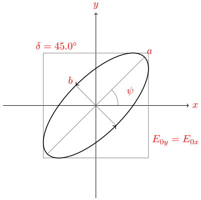

Elliptical pol.

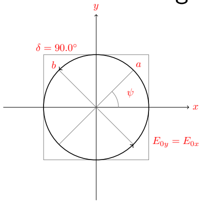

Circle pol.

Interferometric measurement system

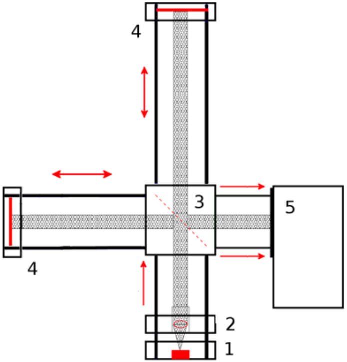

1 - diode laser, **2** - collimator, **3** - beamsplitter 50/50, **4** - mirrors, **5** - detector

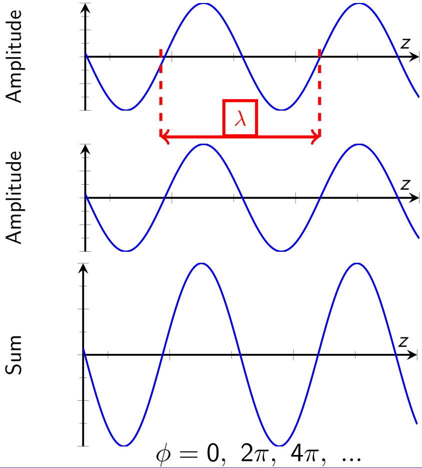

Interferometric measurement system

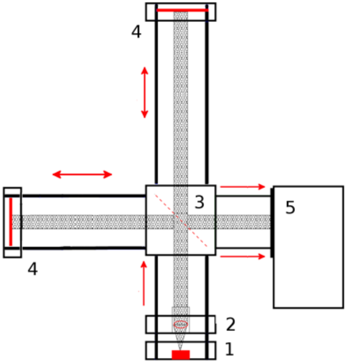

1 - diode laser, **2** - collimator, **3** - beamsplitter 50/50, **4** - mirrors, **5** - detector

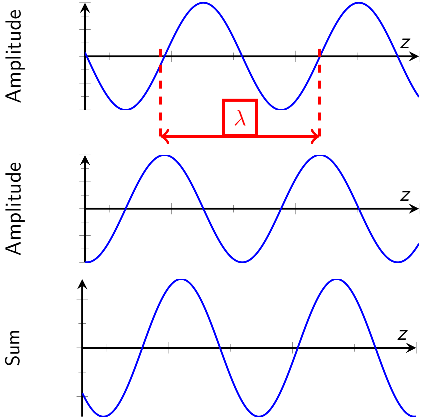

$$\phi = \frac{\pi}{2}, \frac{3\pi}{2}, \ldots$$

Interferometric measurement system

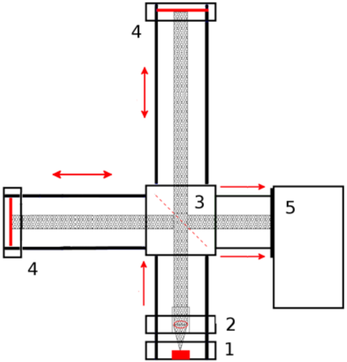

1 - diode laser, **2** - collimator, **3** - beamsplitter 50/50, **4** - mirrors, **5** - detector

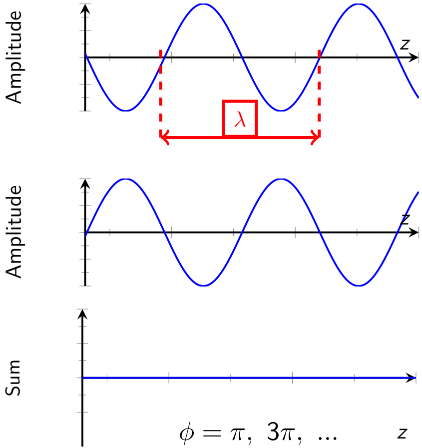

Interferometric measurement system

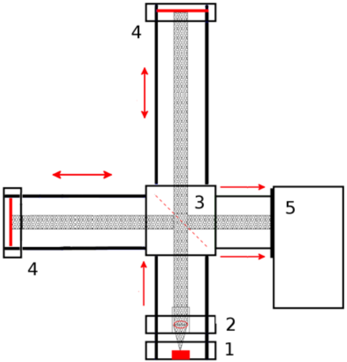

1 - diode laser, **2** - collimator, **3** - beamsplitter 50/50, **4** - mirrors, **5** - detector

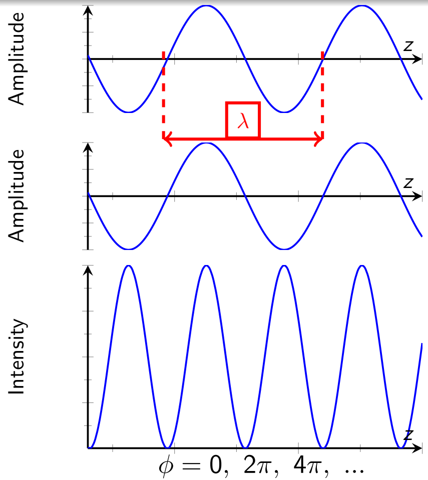

Interferometric measurement system

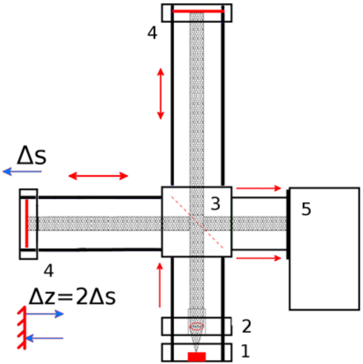

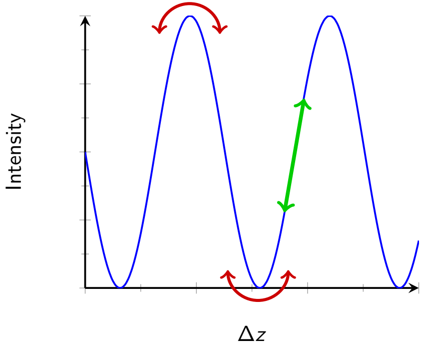

1 - ldiode laser, **2** - collimator, **3** - beamsplitter 50/50, **4** - mirrors, **5** - detector

Interferometric measurement system

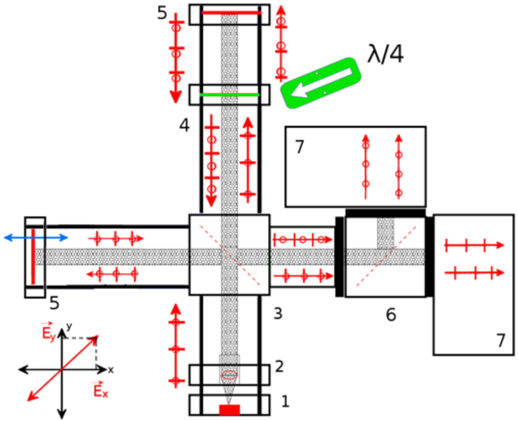

1 - diode laser,

2 - collimator,

3 - beamsplitter 50/50,

4 - phase retarder,

5 - mirrors,

6 - polarized beamsplitter,

7 - detectors.

D. Kucharski, F. Meijer, E. Stachowska, Cz. J. Jermak, Sposób bezstykowego pomiaru odchyłki kształtu metodą interferometryczną, 2013/11/07, Pat/1667 P.405952

Interferometric measurement system

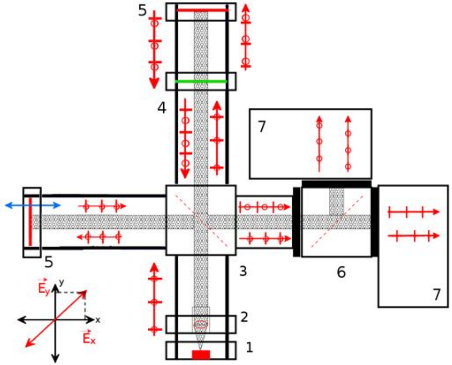

1 - diode laser, **2** - collimator, **3** - beamsplitter 50/50, **4** - phase retarder,

5 - mirrors, **6** - polarized beamsplitter, **7** - detectors

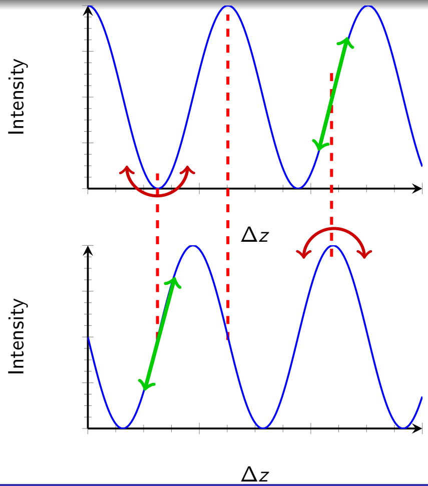

Interferometric measurement system

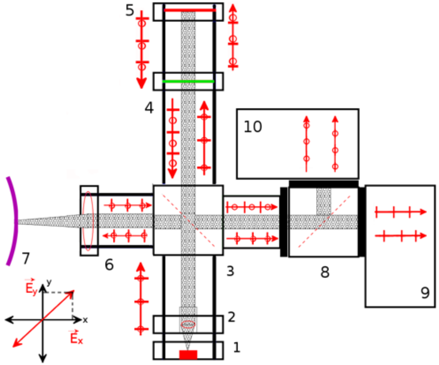

1 - diode laser, **2** - collimator, **3** - beamsplitter 50/50, **4** - phase retarder,

5 - mirrors, **6** - polarized beamsplitter, **7** - detectors

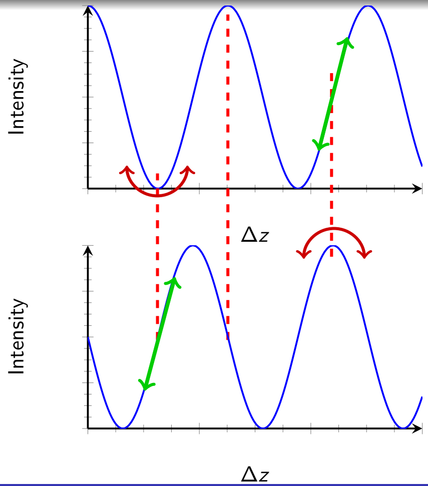

System construction

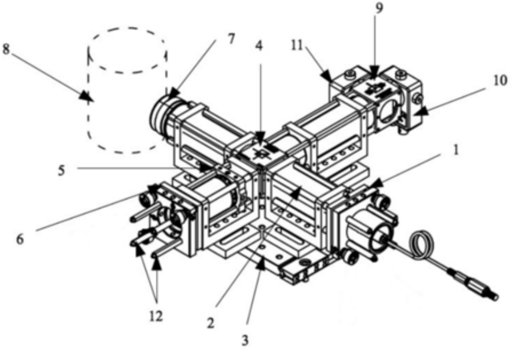

1 - semiconductor laser 532 nm, **2** - tubes with collimator, **3** - translation stage, **4** - beamsplitter 50/50, **5** - phase retarder, **6** - mirror, **7** - regulation lens, **8** - object to measure, **9** - polarized beamsplitter, **10-11** - photodetectors, **12** - rods

D. Kucharski, F. Meijer, E. Stachowska, Cz. J. Jermak, Układ do interferometrycznego, bezstykowego pomiaru odchyłki kształtu, 2014/05/04, Pat/1695 P.408075

System construction

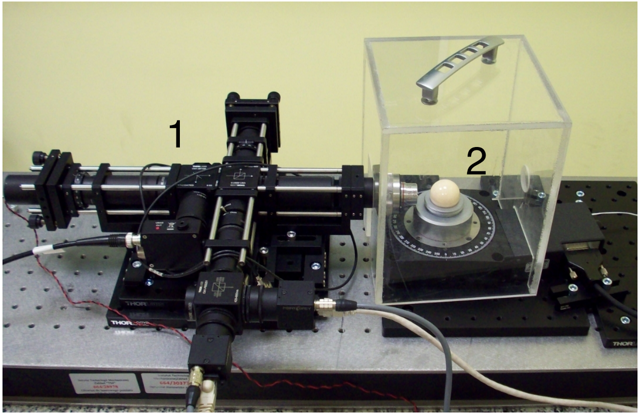

1 - Modified Twyman-Green interferometer, **2** - Rotation stage with object to measure

Example data

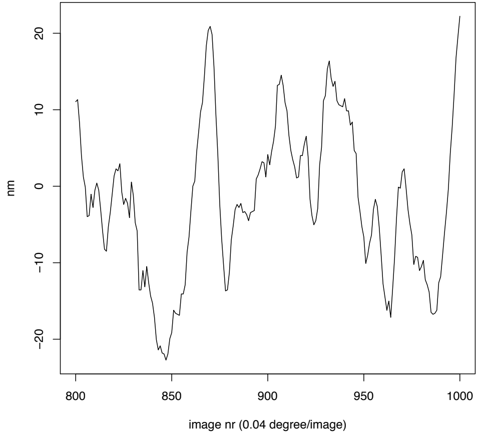

Digital holographic microscopy (DHM)

Mieczysław Wolfke (1883 – 1947)

Denis Gabor (1900 – 1979). Nobel prize in 1971

Digital holographic microscopy (DHM)

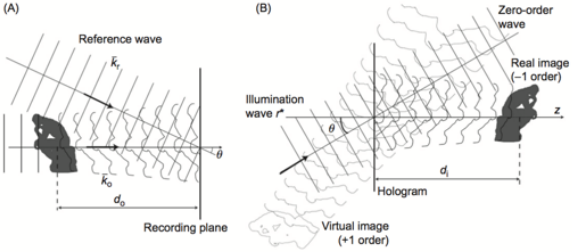

Principle of off-axis (A) recording and (B) reconstruction in DHM. A hologram resulting from the interference of the reference and object waves is recorded on the camera (in the recording plane) with a small incident angle, θ. For the reconstruction process, the hologram is digitally re-illuminated and the zero order is filtered to obtain a complete representation of the wave front (both in terms of intensity and phase) originally emitted by the object

source: B. Rappaz, C. Depeursinge, P. Marquet, N. Shaked, CHAPTER 5. Digital Holographic Microscopy for Measuring Biophysical Parameters of Living Cells, First Edition, Elsevier Inc, 2012. doi:10.1016/B978-0-12-415871-9.00005-3.

DHM by Lyncée tec

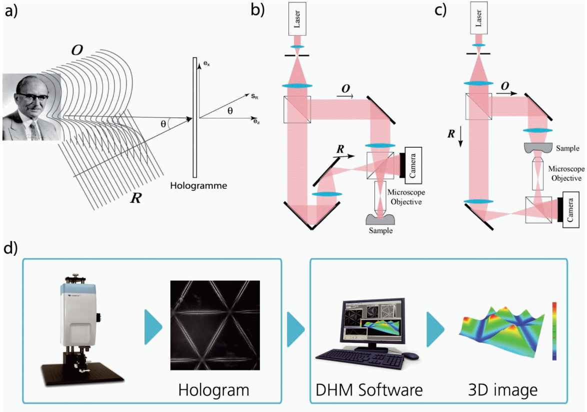

a) Basics, b) DHM reflectometer, c) DHM transmision, d) data evaluation [image source]

DHM by Lyncée tec

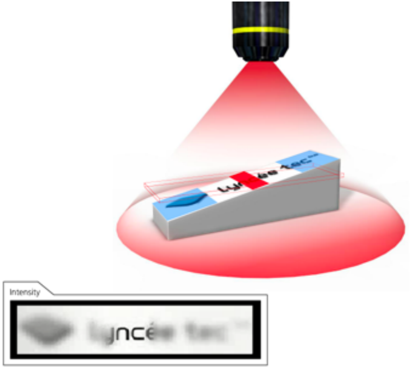

Classical microscopy [image source]

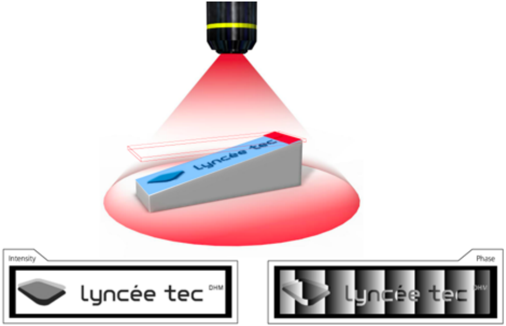

DHM [image source]

DHM by Lyncée tec

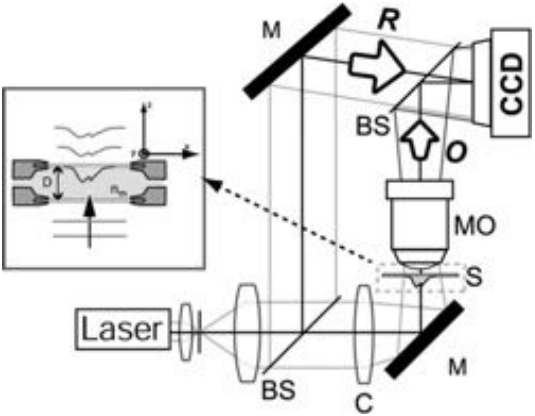

[image source]

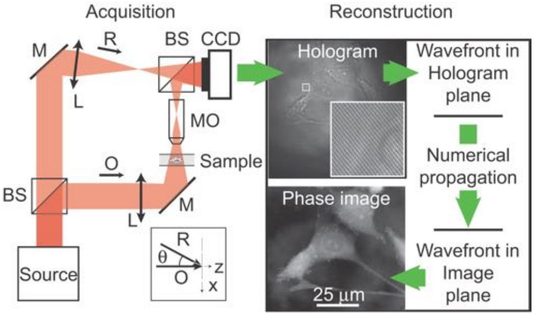

[image source]

DHM – example data

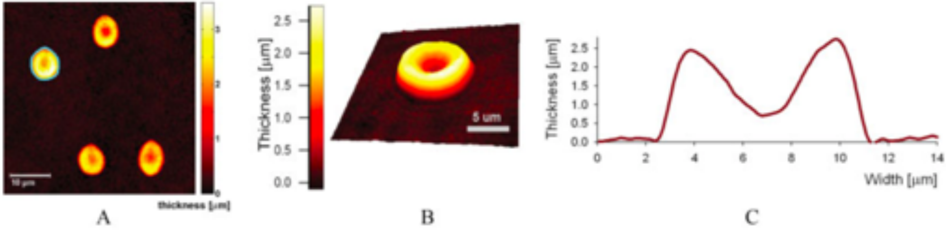

(A) Thickness distribution of human erythrocytes. The cell contour (light blue line) is determined by a classical gradient-based edge detection algorithm. The mean refractive index and the measured volume of selected cells are: n 5 1.396 and v 5 99.3 fl, respectively. (B) Pseudo 3D representation of the cell thickness of an erythrocyte (raw image). (C) Thickness profile obtained in central cross-section of the cell

source: B. Rappaz, A. Barbul, Y. Emery, R. Korenstein, C. Depeursinge, P.J. Magistretti, et al., Comparative study of human erythrocytes by digital holographic microscopy, confocal microscopy, and impedance volume analyzer, Cytometry. 73A (2008) 895–903. doi:10.1002/cyto.a.20605.

DHM – example data

Red Blood Cell, membranes fluctuations [image source]

DHM – example data

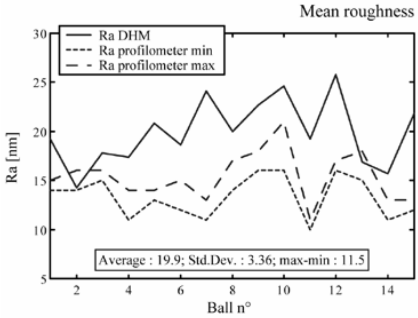

Mean roughness (Ra) measurements on 15 micro-balls of 1 mm diameter.

source: F. Montfort, Y. Emery, E. Solanas, E. Cuche, N. Aspert, P. Marquet, et al., Surface roughness parameters measurements by digital holographic microscopy (DHM), in: Third International Symposium on Precision Mechanical Measurements, SPIE, 2006: pp. 62800V–62800V–6. doi:10.1117/12.716113.

DHM – example data

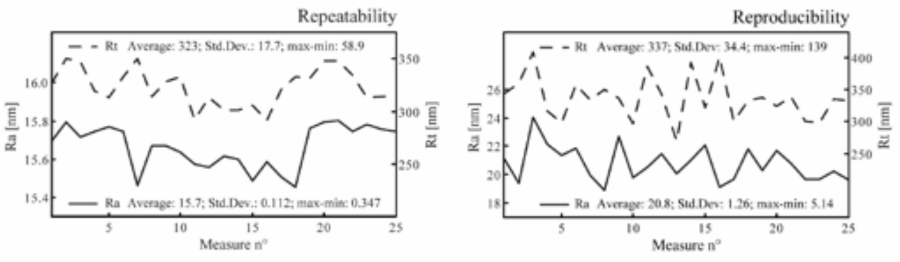

Repeatability and reproducibility tests. The repeatability is performed by 25 measurements on the same surface and the reproducibility by 25 measurements on the different areas of a same micro-ball.

source: F. Montfort, Y. Emery, E. Solanas, E. Cuche, N. Aspert, P. Marquet, et al., Surface roughness parameters measurements by digital holographic microscopy (DHM), in: Third International Symposium on Precision Mechanical Measurements, SPIE, 2006: pp. 62800V–62800V–6. doi:10.1117/12.716113.

DHM – example data

Droplet evaporation [image source]

DHM - configuration

	T1000	T2100
Configuration	One laser source	Two laser sources
Measurement modes	Single wavelength	Single and dual wavelength
Accuracy (as demonstrated by taking the temporal standard deviation on 1 pixel over 30 measurements)	1.0 nm 1	1.0 / 5.0 nm 1 *
Vertical resolution (defined as twice the accuracy)	2.0 nm 1	2.0 / 10.0 nm 1 *
Repeatability (as demonstrated by taking the one sigma Rq value of 30 repeatability measurements on SiC reference mirror)	0.02 nm 1	0.02 / 0.05 nm 1 *
Vertical measuring range (without any scanning)	› up to 500 µm for continuous structures	› up to 500 µm for continuous structures
Max. height of steps with sharp edges (Depends on the laser source(s) and operating wavelength(s))	› up to 1 µm 1 › up to 3.5 µm 2	› up to 7 µm 1 › up to 22 µm 2

1 Converted value for measurements in air and with sample refractive index n=1.5
2 Converted value for measurements in water and with sample refractive index n=1.5
* With / Without single wavelength mapping

Distinctiveness between the two series of DHM [image source]

Non-destructive testing - shearography

Shearography – Speckle pattern shearing interferometry

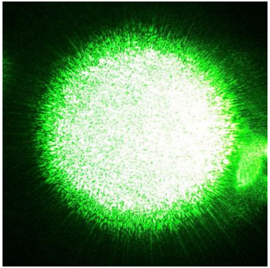

Laser speckle on a digital camera image from a green laser pointer. This is a subjective speckle pattern [image source]

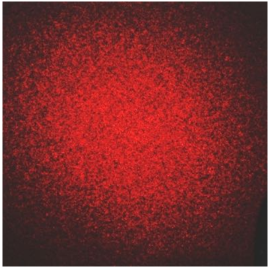

A photograph of an objective speckle pattern. This is the light field formed when a laser beam was scattered from a plastic surface onto a wall [image source]

Non-destructive testing - shearography

„Shearography is an interferometric technique developed to address several limitations of holography. Its significant advantages include (1) not requiring a reference light beam, thus leading to simple optical setups, reduced coherence length requirement of the laser, and lax vibration isolation and (2) direct measurement of surface strains (first-order derivatives of surface displacements). These distinct advantages have rendered shearography as a practical measurement tool and it has already gained wide industrial acceptance for non-destructive testing [1]."

[1] Y.Y. Hung, H.P. Ho, Shearography: An optical measurement technique and applications, Materials Science and Engineering: R: Reports. 49 (2005) 61–87. doi:10.1016/j.mser.2005.04.001.

Shearography – setup

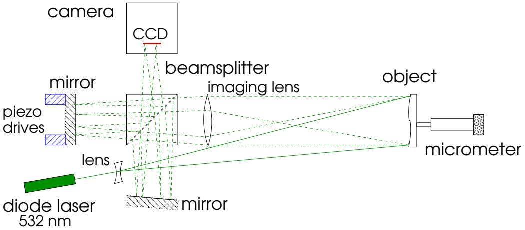

The optical layout [2]

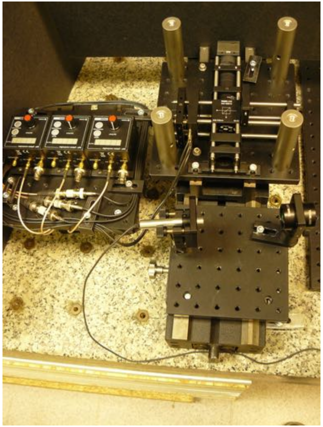

The shearograph [2]

[2] Meijer, F., K. Bula, D. Kucharski, and E. Stachowska. "Non-destructive Deformation Measurements and Defect Testing of Polymer Structures". In: The 24th Annual World Forum on Advanced Materials. Poznan, Poland

Shearography – setup

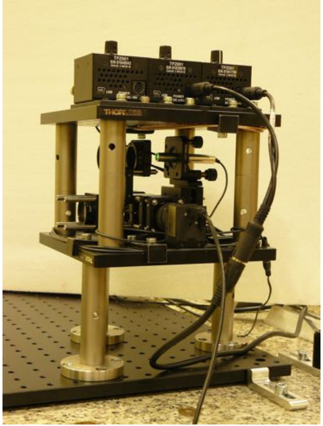

The compact shearograph

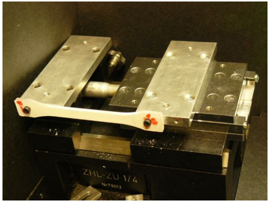

Loading by pulling

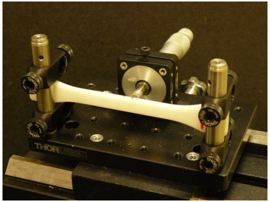

Loading by pushing the sample in the centre

Shearography – example data

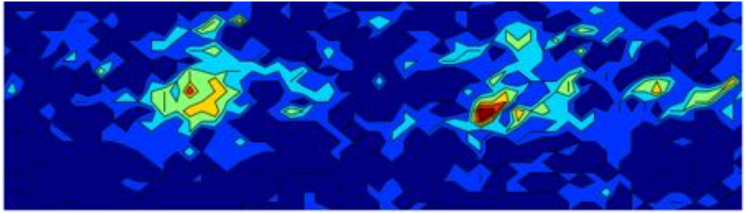

In this contour plot of an elongated sample the smallest differences between two pictures are in dark blue, the largest differences are in red, corresponding to the larger two holes [2]

[2] Meijer, F., K. Bula, D. Kucharski, and E. Stachowska. "Non-destructive Deformation Measurements and Defect Testing of Polymer Structures". In: The 24th Annual World Forum on Advanced Materials. Poznan, Poland

Shearography – example data

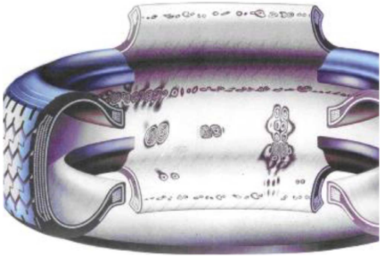

Shearographic fringe pattern revealing separation along the steel belt-edge of a truck tire [1]

[1] Y.Y. Hung, H.P. Ho, Shearography: An optical measurement technique and applications, Materials Science and Engineering: R: Reports. 49 (2005) 61–87. doi:10.1016/j.mser.2005.04.001.

Shearography – example data

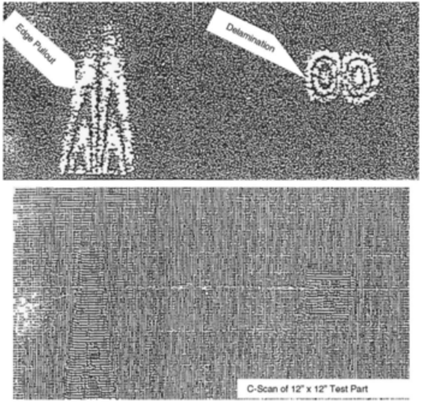

Comparison of shearography with C-scan ultrasound. An edge pullout and a delamination in a composite panel are revealed by both techniques. Time required: 10 min for ultrasound and 1 s for shearography. Moreover, fluid coupling is needed in ultrasonic testing [1]

Shearography solutions

Q-810 Vacuum Hood Shearography [image source]

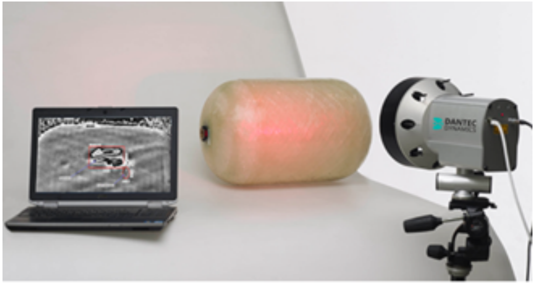

Portable, compact and robust Laser Shearography inspection system that takes NDT & Quality Control to a new level [image source]

Laser vibrometry in the NDT

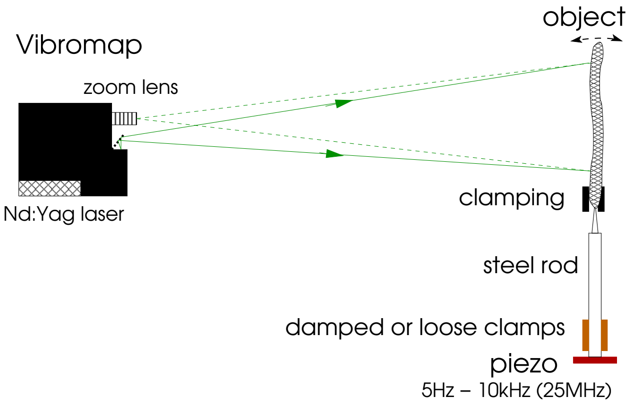

The scheme of the vibrometer layout [2]

Setup

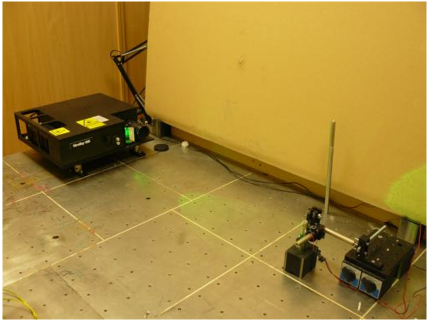

The experimental set-up. The Vibromap to the left and a sample holder to the right

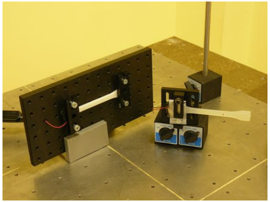

A sample holder

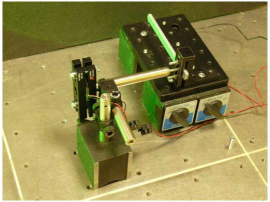

A sample holder

Example data

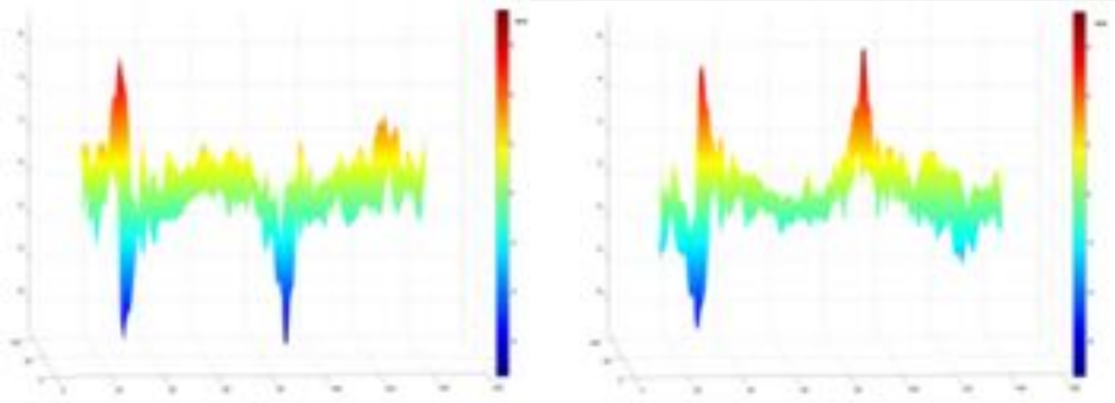

Vibration profile of a sample with two holes at the backside visible, at two moments of the vibration, about half a period apart. The amplitude of the vibration is about 6 nm

Example data

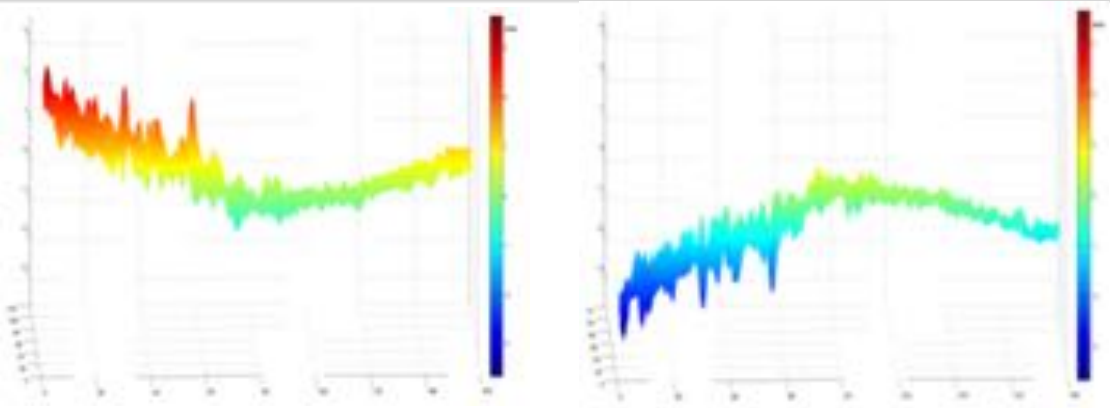

A sample with a partially glued metal plate at the backside, at two different times during the vibration. The amplitude is about 3 nm. The measured part is about 80 mm long

Laser vibrometry solutions by Optonor AS

VibroMap 1000 [image source]

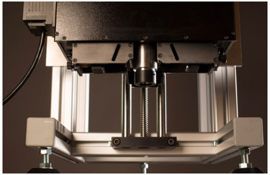

MEMSMap 510 [image source]

SNT 410 [image source]

Interferograms analysis

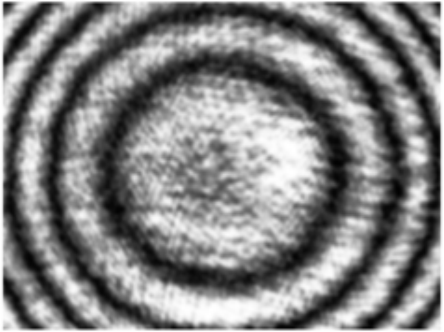

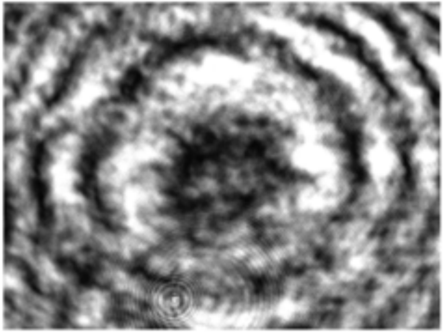

Interferograms analysis

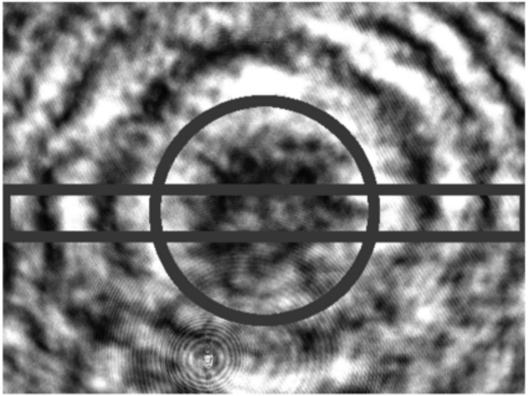

Interferograms analysis

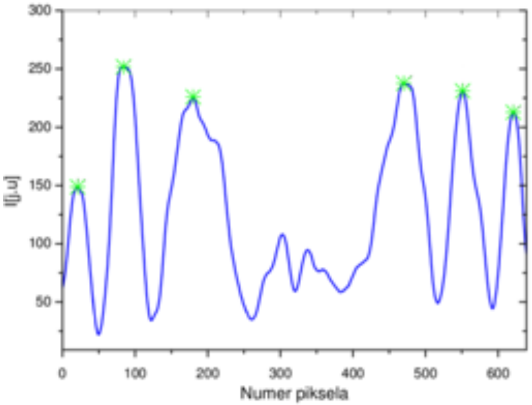

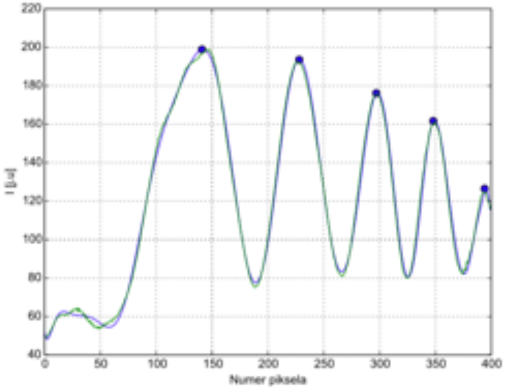

Phase determination

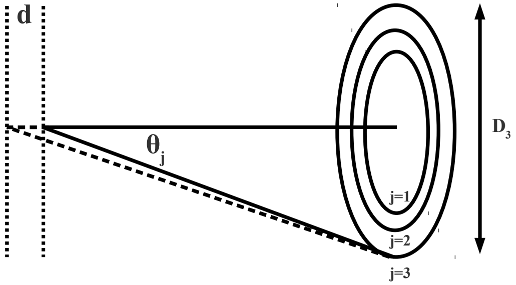

d – distance between sources.

$$\phi = \frac{\pi}{\lambda} 2d \cos\theta.$$

$$I \propto \cos^2\left(\frac{\pi}{\lambda} 2d \cos\theta\right). \quad (1)$$

Intensity is max, when

$$p_\theta = \frac{2d cos\theta}{\lambda}, \quad (2)$$

Phase determination

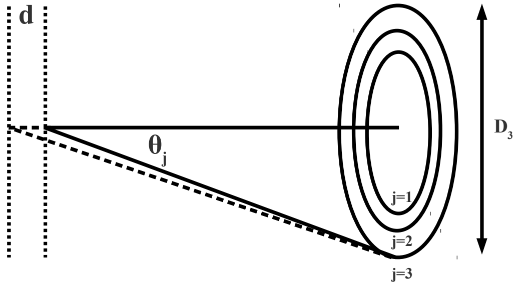

$$\frac{2d\cos\theta_j}{\lambda} = p - j + 1. \qquad (3)$$

$$p + \epsilon = \frac{2d}{\lambda}. \qquad (4)$$

$$(p + \epsilon)\cos\theta_j = p - j + 1. \qquad (5)$$

$$mD_j = 2\theta, \qquad (6)$$

$$cos\theta_j = 1 - \frac{{\theta_j}^2}{2} = 1 - \frac{m^2 {D_j}^2}{8}. \qquad (7)$$

Phase determination

$$(p+\epsilon)\cos\theta_j = p - j + 1.$$

$$mD_j = 2\theta,$$

$$cos\theta_j = 1 - \frac{{\theta_j}^2}{2} = 1 - \frac{m^2 {D_j}^2}{8}.$$

$$(p+\epsilon) - (p+\epsilon)\frac{m^2 {D_j}^2}{8} = p - j + 1, \tag{8}$$

or

$$\frac{p+\epsilon}{8} m^2 {D_j}^2 = j + \epsilon - 1 \tag{9}$$

$$for \;\; {D_j}^2 = 0 \;\Rightarrow\; j = 1 - \epsilon. \tag{10}$$

Phase determination

$$d_n - d_0 = \left(\Delta p_n + \Delta\epsilon \right) \frac{\lambda}{2} \tag{11}$$

- No error
- Error in ϵ_n

$$\Delta d = \frac{\lambda}{2} \Delta\epsilon \tag{12}$$

Phase determination

$$d_n - d_0 = \left(\Delta p_n + \Delta \epsilon \right) \frac{\lambda}{2} \tag{11}$$

- No error → Δp_n
- Error in ϵ_n → $\Delta \epsilon$

$$\Delta d = \frac{\lambda}{2} \Delta \epsilon \tag{12}$$

ϵ suite

$$\frac{p+\epsilon}{8} m^2 {D_j}^2 = j + \epsilon - 1$$

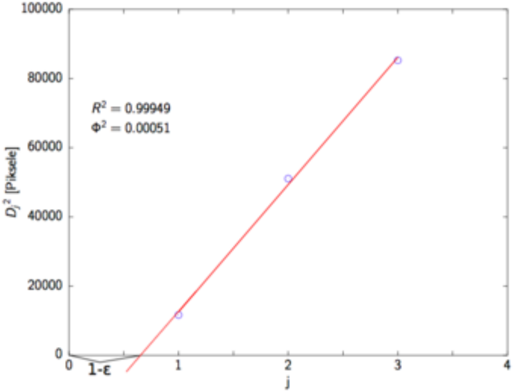

$$\Delta d = \frac{\lambda}{2} \Delta\epsilon$$

Shearography image analysis

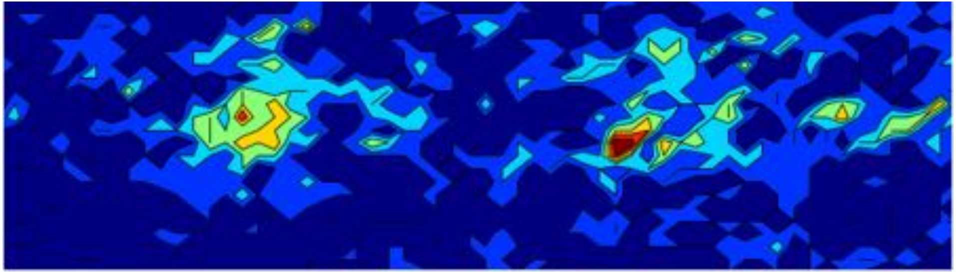

Shearography image analysis

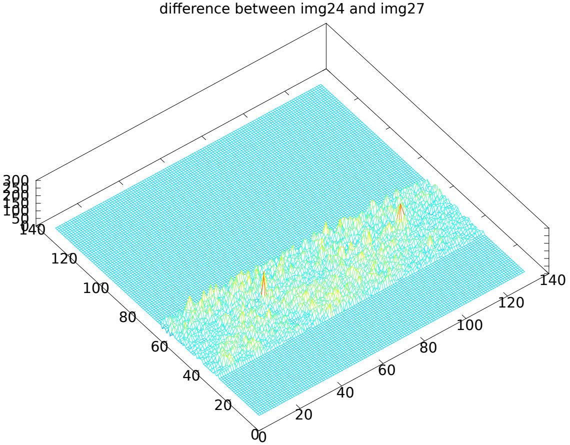

VibroMap data analysis

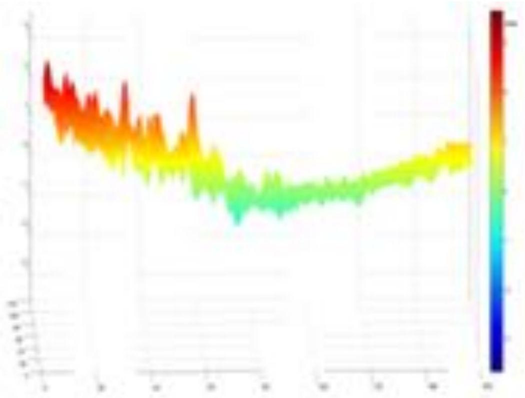

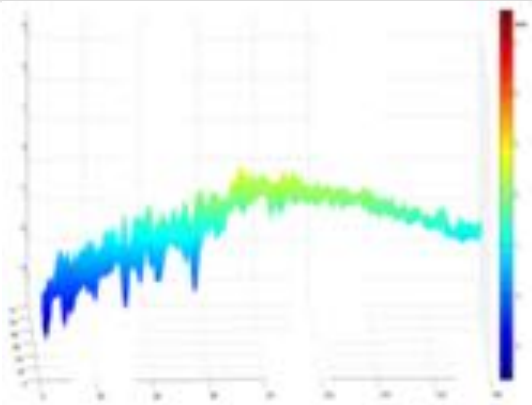

A sample with a partially glued metal plate at the backside, at two different times during the vibration. The amplitude is about 3 nm. The measured part is about 80 mm long

Motywacja

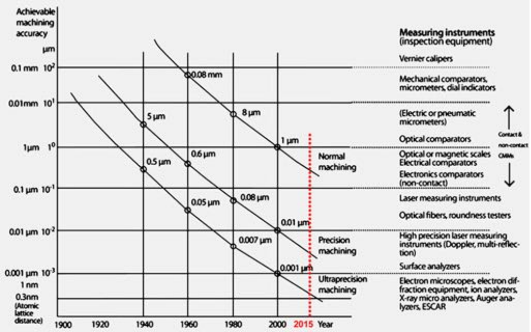

Norio Taniguchi, *On the Basic Concept of 'Nano-Technology'*, Proc. Intl. Conf. Prod. Eng. Tokyo, Part III, Japan Society of Precision Engineering 1974

Exam Q

1. Budowa i zasada działania cyfrowych mikroskopów holograficznych
2. Budowa i zasada działania interferometrycznych systemów pomiarowych, wykorzystywanych w badaniach tekstury powierzchni.
3. Shearografia w badaniach NDT.
4. Laserowa wibrometria w badaniach NDT.
5. Na czym polega analiza obrazów we współczesnych optycznych systemach pomiarowych ? – przykłady.
6. Kalibracja laserowych systemów pomiarowych.
7. Porównanie OSP ze stykowymi systemami pomiarowymi pod kątem zdolności rozdzielczej i obszaru zastosowań.

Thank You !